Sound & Vibration 2026, 60(3), 4116.
doi: https://doi.org/10.59400/sv4116

Article

Hidden-state unscented Kalman filter with unknown input for the joint identification of 3D structural parameters and unknown excitation

Lijun Liu[1], Yahan Yang[1], Shoujin Chen[1], Shiyu Wang[1], Ying Lei[1,2], Yujue Zhou[3], Nan Gong[1,*]

[1] Department of Civil Engineering, Xiamen University, Xiamen 361005, China
[2] Xiamen Key Laboratory of Integrated Application of Intelligent Technology for Architectural Heritage Protection, Xiamen University, Xiamen 361005, China
[3] Architecture Engineering Institute, Sanming University, Sanming 365004, China
*** Corresponding author:** Nan Gong, gongnan@xmu.edu.cn

CITATION

Liu L, Yang Y, Chen S, et al. Hidden-state unscented Kalman filter with unknown input for the joint identification of 3D structural parameters and unknown excitation. Sound & Vibration. 2026; 60(3): 4116. https://doi.org/10.59400/sv4116

ARTICLE INFO

Received: 2 March 2026
Revised: 3 April 2026
Accepted: 9 April 2026
Available online: 18 May 2026

Abstract: The unscented Kalman filter with unknown input (UKF-UI) is an effective method for the identification of structural system and unknown excitation, but for three-dimensional multi-degree-of-freedom structures, the joint identification of structural state-parameter-unknown excitation often leads to high dimensions of extended state vector. To address this issue, a hidden-state unscented Kalman filter with unknown input is proposed for the joint identification of structural parameters and unknown excitation of three-dimensional structures. In the proposed method, only the time-invariant structural parameters are included in the structural state vector, while the displacements and velocities of all structural degrees of freedom are defined as hidden states and excluded from the state vector. This explicitly avoids the conventional extended state vector containing displacement, velocity and structural parameters. By reducing the state vector dimension, the identification of joint structural state-parameter is reduced to parameter-only identification. Moreover, the unbiased minimum variance estimation is used to achieve synchronous identification of unknown excitation. It avoids prior assumptions about unknown excitation and enhances the applicability in practical engineering. The identification of a three-dimensional frame structure under unknown excitation is used to verify the effectiveness of the proposed method. Through the observation of partial acceleration and displacement response data, structural element parameters of the three-dimensional structure and the unknown excitation acting on the three-dimensional structure can be identified.

Keywords: unknown excitation; unscented Kalman filter; system parameter identification; three-dimensional structure; unknown excitation identification

1. Introduction

In the course of the long-term operation of engineering structures, structural damage and material deterioration gradually develop due to construction deficiencies, human activities, environmental actions, and the combined effects of various service loads. The rapid development of structural health monitoring (SHM) has provided significant technical support for achieving the above safety objectives. It's a key technology for evaluating the performance, safety, and durability of structures through real-time or periodic monitoring and analysis of their dynamic responses [1, 2]. Structural damage generally causes variations in physical properties, such as stiffness and damping, and these variations are typically reflected in the vibration characteristics of the structure. System identification has long been regarded as an important approach for nondestructive detection of structural damage. Numerous system identification methods have been developed, including the extended Kalman Filter [3, 4], Hilbert Transform [5], Wavelet Algorithm [6], Recursive Subspace Algorithm [7], and Bayesian Filter [8].

Precise identification of structural parameters enables an effective determination of the specific location and degree of structural damage, thereby making it a core technology for assessing the in-service performance of engineering structures. In the context of structural parameter identification, Kalman filter-based methods [9,10] have been widely adopted as mature approaches and have demonstrated good identification accuracy in many applications. For a linear system, the Kalman filter employs the current observations and the minimum mean square error criterion to recursively update the state estimate. The extended Kalman filter (EKF) [3] extends the Kalman filter by incorporating structural parameters into the state vector, such that the structural parameters can be updated for parameter identification while the system states are being estimated [11]. Some scholars conducted joint identification of structural parameters and unknown input using EKF. Yang et al. [12] developed the Extended Kalman Filter with Unknown Input (EKF-UI) method to identify structural parameters and unmeasurable excitation, deriving an analytical solution. He et al. [13,14] developed a time-domain approach centered on extended Kalman filter theory for joint identification of structural parameters and state vectors under unknown loads, and estimated optimal control forces for vibration suppression based on the identification results. Huang et al. [15] proposed an adaptive generalized extended Kalman filter with unknown input (AGEKF-UI) by fusing the zero-order-hold assumption and random walk model for unknown inputs. The authors [16] proposed the smoothing extended Kalman filter with unknown input without direct feedthrough based on the minimum variance unbiased estimation. Zhang et al. [17] proposed an extended Kalman filter method with a forgetting factor matrix and unknown inputs, which enables simultaneous identification of time-varying physical parameters and unknown external excitations of structures via a two-stage design. However, for structures exhibiting strong nonlinearity or involving a large number of degrees of freedom, the linearization errors introduced by the first-order Taylor approximation in the EKF may significantly degrade identification accuracy. The evaluation of the Jacobian matrix is computationally cumbersome, especially for high-dimensional systems.

To overcome these deficiencies, Julier et al. [18, 19] developed an Unscented Kalman Filter (UKF), which approximates the nonlinear function through probability density and avoids linearizing the nonlinear function. The method directly handles nonlinear problems through unscented transformation. Unscented Kalman filtering approximates the probability distribution of the system by selecting a set of sampling points called Sigma points. These points are symmetrically distributed around the current state's mean and can capture the nonlinear variation characteristics of the state. These points are passed through the nonlinear model to obtain the transformed points. Based on the transformed points, the mean and covariance are recalculated to more accurately describe the distribution after the nonlinear transformation. Unlike the EKF, UKF does not need to calculate the Jacobian matrix and Taylor expansion, avoiding the errors caused by linearization. Sigma points can more realistically reflect the statistical characteristics after nonlinear transformation, and the approximation provided has second-order accuracy. It is more reliable for estimating complex systems and can also be applied to strongly nonlinear systems. Existing research has shown that UKF has certain advantages in the field of structural parameter identification.

The traditional EKF and UKF methods require the known external input excitation to identify nonlinear systems. However, it is difficult to measure all the external excitation under the operating conditions of the engineering structure. It is particularly important to develop a method for jointly identifying the structural parameters and unknown excitation. Ding et al. [20] decomposed the excitation and then carried out system identification, approximating the structural excitation time history by orthogonal decomposition method. Under this approximation, the problem of external excitation identification is transformed into a parameter identification problem. Al-Hussein and Haldar [21] introduced substructures for large-scale structural system identification, combining the unscented Kalman filter with the iterative least squares method for unknown inputs (ILS-UI). Subsequently, this method was extended to three-dimensional structures, and the numerical verification results showed that this method can identify the location and severity of defects in three-dimensional large-scale structural systems at the local element level. Guo et al. [22] assumed that the unknown excitation is a process noise and extended it into the state vector, and used singular value decomposition instead of Cholesky decomposition to improve the robustness of the UKF method. Zheng et al. [23] derived a recursive formulation for unknown-input systems within the conventional unscented Kalman filter framework, and proposed a method to estimate structural unknown inputs by minimizing the observation residuals and solving the associated nonlinear equations. The authors [24] proposed an identification method that combines the unknown-input unscented Kalman filter (UKF-UI) with the nonlinear least-squares method. This method fused displacement and acceleration measurement data to solve the drift phenomenon caused by the recursive state input in nonlinear systems. The proposed UKF-UI method was further extended to the joint identification of large-scale structural parameters and unknown loads. However, in the above research process, the structural state vector contains the displacement, velocity responses of all degrees of freedom and structural parameters. In a structural system with a large number of degrees of freedom, this method will lead to a too high dimensionality of the state vector, thus reducing the identification effect of the filtering algorithm. To address this limitation, this paper hides the displacements and velocity responses at all structural degrees of freedom. The state vector only contains the structural parameters. Thus, it is applicable for parameter identification of three-dimensional multi-degree-of-freedom structures and is conducive to the convergence of the algorithm.

Additionally, some researchers proposed parameter-only identification methods applicable to complex multi-degree-of-freedom systems. Astroza et al. [25] combined the unknown structural parameters to be identified with the unknown input into an augmented state vector and assumed that the recursive process of the unknown input in the time domain conforms to the random walk model. Castiglione et al. [26] proposed a method using a time-varying autoregressive model to describe the unknown input time history, assuming that its model parameters change randomly in the time domain. They used the unscented Kalman filter method to jointly estimate the time-varying autoregressive model parameters and the finite element model parameters of a three-dimensional steel frame structure. This method realized the reconstruction of the ground motion input. The above research often needs to make certain assumptions about the time evolution of the unknown excitation to identify the unknown excitation. For example, the unknown excitation is assumed to be a process noise extended into the state vector. Because the noise covariance matrix has time-varying characteristics, there may be coupling effects when the structural parameters are jointly identified with the unknown excitation. These assumptions have certain limitations for the joint identification of system parameters and unknown input.

This paper proposes a hidden-state UKF-UI method for the joint identification of three-dimensional structural parameters and unknown excitation. In this method, the displacements and velocities of all degrees of freedom of the three-dimensional structure are defined as hidden states. The method modifies the state vector, which originally includes displacements, velocities, and structural parameters at all degrees of freedom of the structure, to only include structural parameters, thereby reducing the dimension of the state vector. The dynamic response states are not used as state variables for sigma point sampling, state prediction, and update in the recursive process. It uses the unbiased minimum variance estimation method to identify unknown excitation, avoiding the need for prior assumptions about the temporal evolution of unknown excitation. Thus, it can jointly identify the parameters and unknown excitation of three-dimensional multi-degree-of-freedom structures.

The innovative points of the article are as follows:

(1) The extended state vector includes only structural parameters to be identified, while structural state variables (such as displacement and velocity) are excluded. As a result, the joint state-parameter estimation problem is transformed into a pure parameter estimation problem, fundamentally overcoming the high-dimensional extended state vector in the conventional Unscented Kalman filter-based structural identification approaches.

(2) A novel joint identification methodology for structural parameters and unknown input based on hidden-state UKF is proposed, which requires no prior assumptions regarding the unknown external excitation.

(3) The structural state can be subsequently estimated based on the joint identification of structural state-unknown excitation by the hidden-state UKF.

2. Derivation of the proposed method

For a linear structure under external excitation, its motion equation is:

$$\boldsymbol{M}\ddot{\boldsymbol{x}}(t) + \boldsymbol{C}(\boldsymbol{\theta})\dot{x}(t) + \boldsymbol{K}(\boldsymbol{\theta})x(t) = \boldsymbol{\eta}^u \boldsymbol{f}^u(t), \tag{1}$$

where $\boldsymbol{M}$ is the mass matrix, $\boldsymbol{C}$ is the damping matrix, $\boldsymbol{K}$ is the stiffness matrix, $\boldsymbol{\theta}$ is the vector of unknown structural parameters to be identified, such as damping parameters and stiffness parameters, and $\boldsymbol{\theta}$ is the time-invariant vector, $\dot{\boldsymbol{\theta}} = 0$, $\boldsymbol{M}$ is regarded as being constant and not dependent on $\boldsymbol{\theta}$, $\ddot{\boldsymbol{x}}$, $\dot{\boldsymbol{x}}$ and $\boldsymbol{x}$ represent the acceleration, velocity, and displacement responses respectively, $\boldsymbol{f}^u$ is the unknown external excitation vector, $\boldsymbol{\eta}^u$ is the localization matrix associated with $\boldsymbol{f}^u$.

Equation (1) can be rewritten as a continuous state-space equation:

$$\begin{aligned}\begin{Bmatrix}\dot{\boldsymbol{x}}(t)\\ \ddot{\boldsymbol{x}}(t)\end{Bmatrix} &= \begin{Bmatrix}\dot{\boldsymbol{x}}(t)\\ -\boldsymbol{M}^{-1}\boldsymbol{C}(\boldsymbol{\theta})\dot{\boldsymbol{x}}(t)-\boldsymbol{M}^{-1}\boldsymbol{K}(\boldsymbol{\theta})\boldsymbol{x}(t)\end{Bmatrix} + \begin{Bmatrix}0\\ \boldsymbol{M}^{-1}\boldsymbol{\eta}^u\end{Bmatrix}\boldsymbol{f}^u(t)\\ &= \boldsymbol{G}\left(\boldsymbol{x}(t),\dot{\boldsymbol{x}}(t),\boldsymbol{\theta}\right)+\boldsymbol{D}\boldsymbol{f}^u(t)\end{aligned}, \tag{2}$$

where $\boldsymbol{G}\left(\boldsymbol{x}(t),\ \dot{\boldsymbol{x}}(t),\boldsymbol{\theta}\right) = \begin{Bmatrix}\dot{\boldsymbol{x}}(t)\\ -\boldsymbol{M}^{-1}\boldsymbol{C}\left(\boldsymbol{\theta}\right)\dot{\boldsymbol{x}}(t)-\boldsymbol{M}^{-1}\boldsymbol{K}\left(\boldsymbol{\theta}\right)x(t)\end{Bmatrix}$; $\boldsymbol{D} = \begin{Bmatrix}0\\ \boldsymbol{M}^{-1}\boldsymbol{\eta}^u\end{Bmatrix}$.

The structural system is a feed-through structural system, and the observation equation contains a direct feed-through term of the unknown input. Therefore, the discrete-time observation equation can be written as:

$$\begin{aligned}\boldsymbol{y}_{k+1} &= \boldsymbol{L}\begin{Bmatrix}\ddot{\boldsymbol{x}}_{k+1}\\ \boldsymbol{x}_{k+1}\end{Bmatrix}\\ &= \boldsymbol{L}\begin{Bmatrix}-\boldsymbol{M}^{-1}\boldsymbol{K}\left(\boldsymbol{\theta}_k\right)\boldsymbol{x}_{k+1}-\boldsymbol{M}^{-1}\boldsymbol{C}\left(\boldsymbol{\theta}_k\right)\dot{\boldsymbol{x}}_{k+1}\\ \boldsymbol{x}_{k+1}\end{Bmatrix}+\boldsymbol{L}\begin{Bmatrix}\boldsymbol{M}^{-1}\boldsymbol{\eta}^u\\ 0\end{Bmatrix}\boldsymbol{f}^u_{k+1}\end{aligned}, \tag{3}$$

where $\boldsymbol{y}_{k+1}$ is the observation vector and $\boldsymbol{L}$ is the observation localization matrix, the subscript k + 1 indicates the (k + 1)-th discrete-time step, $\boldsymbol{\theta}_k$ is the vector of structural parameters at the k-th time step.

Since the structure state at the step k + 1 is related to the current structural parameters $\boldsymbol{\theta}_{k+1}$, which equals to $\boldsymbol{\theta}_k$, historical external excitation and initial conditions, Equation (3) can be written as:

$$\boldsymbol{y}_{k+1} = \boldsymbol{h}_{k+1}\left(\boldsymbol{\theta}_k,\boldsymbol{f}^u_{0:k},\boldsymbol{x}_0,\dot{\boldsymbol{x}}_0\right)+\boldsymbol{B}\boldsymbol{f}^u_{k+1}, \tag{4}$$

where $\boldsymbol{f}^u_{0:k} = [\boldsymbol{f}^u_0, \boldsymbol{f}^u_1 \cdots \boldsymbol{f}^u_k]$ is the unknown external excitation acting on the structure from step 0 to step k , $\boldsymbol{x}_0,\ \dot{\boldsymbol{x}}_0$ is the initial displacement and velocity of the structural system, $\boldsymbol{h}_{k+1}\left(\boldsymbol{\theta}_k,\boldsymbol{f}^u_{0:k},\boldsymbol{x}_0,\dot{\boldsymbol{x}}_0\right)$ is the response function of the structure at the step k + 1, $\boldsymbol{B} = \boldsymbol{L}\begin{Bmatrix}\boldsymbol{M}^{-1}\boldsymbol{\eta}^u\\ 0\end{Bmatrix}$ is the external excitation positioning matrix.

According to Equation (4), the response of the structure from step 1 to step k + 1 can be obtained:

$$\boldsymbol{y}_{1:k+1} = \begin{bmatrix}\boldsymbol{L} & & \\ & \ddots & \\ & & \boldsymbol{L}\end{bmatrix}\begin{Bmatrix}\ddot{\boldsymbol{x}}_1\\ \boldsymbol{x}_1\\ \vdots\\ \ddot{\boldsymbol{x}}_{k+1}\\ \boldsymbol{x}_{k+1}\end{Bmatrix} = \boldsymbol{h}_{1:k+1}\left(\boldsymbol{\theta}_k,\boldsymbol{f}^u_{0:k},\boldsymbol{x}_0,\dot{\boldsymbol{x}}_0\right)+\overline{\boldsymbol{B}}\boldsymbol{f}^u_{k+1}, \tag{5}$$

where $\boldsymbol{y}_{1:k+1}$ represents the response of the structure from step 1 to step $k+1$, $\boldsymbol{h}_{1:k+1}\left(\boldsymbol{\theta}_k, \boldsymbol{f}_{0:k}^u, \boldsymbol{x}_0, \dot{\boldsymbol{x}}_0\right)$ is the response function of the structure from step 1 to step $k+1$, $\overline{\boldsymbol{B}} = \begin{bmatrix} \boldsymbol{L} & & \\ & \ddots & \\ & & \boldsymbol{L} \end{bmatrix} \begin{Bmatrix} 0 \\ 0 \\ \vdots \\ \boldsymbol{M}^{-1}\boldsymbol{\eta}^u \\ 0 \end{Bmatrix}$, $\boldsymbol{f}_{1:k+1}^u$ represents the excitation from step 1 to step $k+1$.

The steps for identification are as follows:

(1) State equation and observation equation

State equation:

$$\boldsymbol{\theta}_{k+1} = \boldsymbol{\theta}_k + \boldsymbol{w}_k. \tag{6}$$

Observation equation:

$$\boldsymbol{y}_{k+1}^v = \boldsymbol{h}_{k+1}\left(\boldsymbol{\theta}_k, \boldsymbol{f}_{0:k}^u, \boldsymbol{x}_0, \dot{\boldsymbol{x}}_0\right) + \boldsymbol{B}\boldsymbol{f}_{k+1}^u + \boldsymbol{v}_{k+1}, \tag{7}$$

$$\boldsymbol{y}_{1:k+1}^v = \boldsymbol{h}_{1:k+1}\left(\boldsymbol{\theta}_k, \boldsymbol{f}_{0:k}^u, \boldsymbol{x}_0, \dot{\boldsymbol{x}}_0\right) + \bar{\boldsymbol{B}}\boldsymbol{f}_{k+1}^u + \boldsymbol{v}_{1:k+1}, \tag{8}$$

where $\boldsymbol{y}_{k+1}^v$ and $\boldsymbol{y}_{1:k+1}^v$ are the response of the structure after considering the measurement noise.

After considering the modelling error in the state equation, a term $\boldsymbol{w}_k$ is added, whose mean is 0 and variance is $\boldsymbol{Q}$. After considering the measurement error in the observation equation, a term $\boldsymbol{v}_{k+1}$ is added, whose mean is 0, variance is $\boldsymbol{R}$, and $\boldsymbol{v}_{1:k+1} = \left[\boldsymbol{v}_1^{\boldsymbol{T}}, \ \ldots. \ , \boldsymbol{v}_{k+1}^{\boldsymbol{T}}\right]^{\boldsymbol{T}}$, whose mean is 0 and variance is $\boldsymbol{R}_{1:k+1} = diag(\boldsymbol{R}, \ \ldots. \ \boldsymbol{R})$. In this paper, $\boldsymbol{Q}$ and $\boldsymbol{R}$ are supposed to be the constant matrix that are time-invariant.

(2) Recursive process

The state vector $\boldsymbol{\theta}_k$ at the k-th time step, whose mean is $\widehat{\boldsymbol{\theta}}_{k|k} = E\left\{\boldsymbol{\theta}_k\right\}$, the filtering covariance matrix of $\boldsymbol{\theta}_k$ at step k is $\boldsymbol{P}_{k|k}^{\boldsymbol{\theta\theta}} = E\left\{\left(\boldsymbol{\theta}_k - \widehat{\boldsymbol{\theta}}_{k|k}\right)\left(\boldsymbol{\theta}_k - \widehat{\boldsymbol{\theta}}_{k|k}\right)^T\right\}$. To estimate the mean and covariance matrix of $\boldsymbol{\theta}$ at the $(k+1)$-th time step, a set of $2N+1$ sigma points of the k-step state vector are obtained by using the unscented transform as follows:

$$\widehat{\boldsymbol{\theta}}_{i,k|k} = \begin{cases} \widehat{\boldsymbol{\theta}}_{k|k}, \ i = 0 \\ \widehat{\boldsymbol{\theta}}_{k|k} + \left(\sqrt{(N+\lambda)\boldsymbol{P}_{k|k}^{\boldsymbol{\theta\theta}}}\right)_i, \ i = 1, \ldots.N \\ \widehat{\boldsymbol{\theta}}_{k|k} - \left(\sqrt{(N+\lambda)\boldsymbol{P}_{k|k}^{\boldsymbol{\theta\theta}}}\right)_i, \ i = N+1\ldots\ldots2N \end{cases}, \tag{9}$$

where $\widehat{\boldsymbol{\theta}}_{i,k|k}$ is the i-th Sigma point at k-th time step, $\widehat{\boldsymbol{\theta}}_{k|k}$ is filtering estimation of k-th time step, N is the dimension of the state vector (only including structural parameters), $\sqrt{\boldsymbol{P}_{k|k}^{\boldsymbol{\theta\theta}}}$ represents the Cholesky decomposition of the symmetric positive definite matrix $\boldsymbol{P}_{k|k}^{\boldsymbol{\theta\theta}}$, $\left(\sqrt{(N+\lambda)\boldsymbol{P}_{k|k}^{\boldsymbol{\theta\theta}}}\right)_i$ denotes the i-th column of the matrix square root, and $\lambda = \alpha^2(N+\kappa) - N$, $\alpha(0 \leq \alpha \leq 1)$ represents the scaling factor of the sigma points, which determines the spread of the sigma points, α usually takes a relatively small value; κ represents the proportional parameter, generally taking $\kappa = 3 - N$ or 0.

The predicted value $\widetilde{\boldsymbol{\theta}}_{k+1|k}$ of the state vector at step *k* + 1 and the corresponding error covariance matrix $\widetilde{\boldsymbol{P}}^{\boldsymbol{\theta\theta}}_{k+1|k}$ are:

$$\widetilde{\boldsymbol{\theta}}_{i,k+1|k} = \widehat{\boldsymbol{\theta}}_{i,k|k}, \tag{10}$$

$$\widetilde{\boldsymbol{\theta}}_{k+1|k} = \sum\nolimits_{i=0}^{2N} w_i^{(m)} \widetilde{\boldsymbol{\theta}}_{i,k+1|k}, \tag{11}$$

$$\widetilde{\boldsymbol{P}}^{\boldsymbol{\theta\theta}}_{k+1|k} = \sum\nolimits_{i=0}^{2N} w_i^{(c)} (\widetilde{\boldsymbol{\theta}}_{i,k+1|k} - \widetilde{\boldsymbol{\theta}}_{k+1|k})(\widetilde{\boldsymbol{\theta}}_{i,k+1|k} - \widetilde{\boldsymbol{\theta}}_{k+1|k})^T + \boldsymbol{Q}, \tag{12}$$

where $w_i^{(m)}$, $w_i^{(c)}(i = 0, 1, 2 \cdots 2N)$ are the weights associated with the mean and covariance of the sigma points, respectively.

The corresponding weights of the mean and covariance of each sigma point are given by the following formula:

$$\begin{aligned} w_0^{(m)} &= \frac{\lambda}{(N+\lambda)} \\ w_0^{(c)} &= \frac{\lambda}{(N+\lambda)} + (1 + \beta - \alpha^2) \\ w_i^{(m)} = w_i^{(c)} &= \frac{1}{2(N+\lambda)}, i = 1, 2, 3 \cdots 2N, \end{aligned} \tag{13}$$

where β is the non-weight coefficient. For the Gaussian distribution, β generally takes 2.

Since the unknown excitation $\boldsymbol{f}^u_{k+1}$ at step *k* + 1 only affects the structural response at step *k* + 1 and does not affect the previous structural responses, when identifying the unknown excitation $\boldsymbol{f}^u_{k+1}$ at step *k* + 1, only the structural response at step *k* is used. Equation (7) is adopted as the observation equation. In addition, when using $\boldsymbol{h}_{k+1}\left(\boldsymbol{\theta}_{k+1}, \boldsymbol{f}^u_{0:k}, \boldsymbol{x}_0, \dot{\boldsymbol{x}}_0\right)$ to calculate the structural response at step *k*, the unknown excitation from step 0 to step *k* is required. Here, only the uncertainty of the unknown excitation identified at the step *k* + 1 is considered, and the uncertainties of the unknown excitation identified from step 0 to step *k* are not considered. Therefore, when calculating the estimated values of the observation vector $\widetilde{\boldsymbol{y}}_{i,k+1|k}$ at the step *k* + 1, the unknown excitations from step 0 to step *k* use $\widehat{\boldsymbol{f}}^u_{0:k}$:

$$\widetilde{\boldsymbol{y}}_{i,k+1|k} = \boldsymbol{h}_{k+1}\left(\widetilde{\boldsymbol{\theta}}_{i,k+1|k}, \widehat{\boldsymbol{f}}^u_{0:k}, \boldsymbol{x}_0, \dot{\boldsymbol{x}}_0\right), \tag{14}$$

$$\widetilde{\boldsymbol{y}}_{k+1|k} = \sum\nolimits_{i=0}^{2N} w_i^{(m)} \widetilde{\boldsymbol{y}}_{i,k+1|k}. \tag{15}$$

The associated error covariance matrix $\widetilde{\boldsymbol{P}}^{\boldsymbol{yy}}_{k+1|k}$ can be given by:

$$\widetilde{\boldsymbol{P}}^{\boldsymbol{yy}}_{k+1|k} = \sum\nolimits_{i=0}^{2N} w_i^{(c)} (\widetilde{\boldsymbol{y}}_{i,k+1|k} - \widetilde{\boldsymbol{y}}_{k+1|k})(\widetilde{\boldsymbol{y}}_{i,k+1|k} - \widetilde{\boldsymbol{y}}_{k+1|k})^T + \boldsymbol{R}_{k+1}. \tag{16}$$

The unknown excitation $\widehat{\boldsymbol{f}}^u_{k+1|k+1}$ at step $k+1$ obtained according to the unbiased minimum variance estimation method is:

$$\widehat{\boldsymbol{f}}^u_{k+1|k+1}=\left[\boldsymbol{B}^T\left(\widetilde{\boldsymbol{P}}^{\boldsymbol{yy}}_{k+1|k}\right)^{-1}\boldsymbol{B}\right]^{-1}\boldsymbol{B}^T\left(\widetilde{\boldsymbol{P}}^{\boldsymbol{yy}}_{k+1|k}\right)^{-1}(\boldsymbol{y}_{k+1}-\widetilde{\boldsymbol{y}}_{k+1|k}). \tag{17}$$

After obtaining the unknown excitation at step $k+1$ according to Equation (17), the prior estimate value of the state vector is calculated according to the observation Equation (8). The prior estimate values of the state vector are weighted and summed to obtain the estimated value of the observation vector at step $k+1$:

$$\widetilde{\boldsymbol{y}}_{i,1:k+1|k}=\boldsymbol{h}_{1:k+1}(\widetilde{\boldsymbol{\theta}}_{i,k+1|k},\widehat{\boldsymbol{f}}^u_{0:k},x_0,\dot{x}_0), \tag{18}$$

$$\widetilde{\boldsymbol{y}}_{1:k+1|k}=\sum\nolimits_{i=0}^{2N}w_i^{(m)}\widetilde{\boldsymbol{y}}_{i,1:k+1|k}. \tag{19}$$

The covariance $\widetilde{\boldsymbol{P}}^{\boldsymbol{yy}}_{1:k+1|k}$ of the estimated observation vector at step $k+1$, and the cross-covariance matrix $\widetilde{\boldsymbol{P}}^{\boldsymbol{\theta y}}_{1:k+1|k}$ between the state vector and the observation vector can be given by:

$$\widetilde{\boldsymbol{P}}^{\boldsymbol{yy}}_{1:k+1|k}=\sum\nolimits_{i=0}^{2N}w_i^{(c)}[\widetilde{\boldsymbol{y}}_{i,1:k+1|k}-\widetilde{y}_{1:k+1|k}][\widetilde{y}_{i,1:k+1|k}-\widetilde{y}_{1:k+1|k}]^T+\boldsymbol{R}_{1:k+1}, \tag{20}$$

$$\widetilde{\boldsymbol{P}}^{\boldsymbol{\theta y}}_{1:k+1|k}=\sum\nolimits_{i=0}^{2N}w_i^{(c)}[\widetilde{\boldsymbol{\theta}}_{i,k+1|k}-\widetilde{\theta}_{k+1|k}][\widetilde{\boldsymbol{y}}_{i,1:k+1|k}-\widetilde{\boldsymbol{y}}_{1:k+1|k}]^T. \tag{21}$$

Calculate the Kalman gain matrix [27] at step $k+1$ as:

$$\boldsymbol{K}_{1:k+1}=\widetilde{\boldsymbol{P}}^{\boldsymbol{\theta y}}_{1:k+1|k}\left(\widetilde{\boldsymbol{P}}^{\boldsymbol{yy}}_{1:k+1|k}\right)^{-1}\times\left(\boldsymbol{I}-\overline{\boldsymbol{B}}\left(\overline{\boldsymbol{B}}^T\left(\widetilde{\boldsymbol{P}}^{\boldsymbol{yy}}_{1:k+1|k}\right)^{-1}\overline{\boldsymbol{B}}\right)^{-1}\overline{\boldsymbol{B}}^T\left(\widetilde{\boldsymbol{P}}^{\boldsymbol{yy}}_{1:k+1|k}\right)^{-1}\right). \tag{22}$$

Finally, the updated structural parameter state vector $\widehat{\boldsymbol{\theta}}_{k+1|k+1}$ and its related error covariance matrix $\widehat{\boldsymbol{P}}^{\boldsymbol{\theta\theta}}_{k+1|k+1}$ are obtained as:

$$\widehat{\boldsymbol{\theta}}_{k+1|k+1}=\widetilde{\boldsymbol{\theta}}_{k+1|k}+\boldsymbol{K}_{1:k+1}(\boldsymbol{y}_{1:k+1}-\widetilde{\boldsymbol{y}}_{1:k+1|k}), \tag{23}$$

$$\widehat{\boldsymbol{P}}^{\boldsymbol{\theta\theta}}_{k+1|k+1}=\widetilde{\boldsymbol{P}}^{\boldsymbol{\theta\theta}}_{k+1|k}+\boldsymbol{K}_{1:k+1}\widetilde{\boldsymbol{P}}^{\boldsymbol{yy}}_{1:k+1|k+1}\boldsymbol{K}^T_{1:k+1}-\boldsymbol{K}_{1:k+1}\left(\widetilde{\boldsymbol{P}}^{\boldsymbol{\theta y}}_{1:k+1|k}\right)^T-\widetilde{\boldsymbol{P}}^{\boldsymbol{\theta y}}_{1:k+1|k}\boldsymbol{K}^T_{1:k+1}. \tag{24}$$

For the next time step, continue to iterate the updated $\widehat{\boldsymbol{\theta}}_{k+1|k+1}$ and $\widehat{\boldsymbol{P}}^{\boldsymbol{\theta\theta}}_{k+1|k+1}$ in the UKF-UI algorithm.

The algorithm process of hidden-state UKF-UI is summarized as follows (**Algorithm 1**):

Algorithm 1 Process of hidden-state UKF-UI

(1) Set the initial values of the state vector $\boldsymbol{\theta}_{0|0}$, covariance $\boldsymbol{P}_{0|0}$ and unknown input $\boldsymbol{f}_{0|0}$.

(2) Calculate the sigma point of the step k parameter vector and the corresponding weights of the mean and covariance of each sigma point from Equations (9) and (13).

(3) Calculate the predicted value $\widetilde{\boldsymbol{\theta}}_{k+1|k}$ of the step $k+1$ state vector and its corresponding error covariance matrix $\widetilde{\boldsymbol{P}}^{\boldsymbol{\theta\theta}}_{k+1|k}$ according to Equations (10) and (12).

(4) Identify the unknown excitation $\widehat{\boldsymbol{f}}^{u}_{k+1|k+1}$ according to Equations (14)–(17).
(5) The predicted value of the observation vector $\widetilde{\boldsymbol{y}}_{1:k+1|k}$ is obtained according to Equations (18) and (19).
(6) According to Equations (20) and (21), calculate the covariance $\widetilde{\boldsymbol{P}}^{\boldsymbol{yy}}_{\boldsymbol{1:k+1|k}}$ of the estimated value of the observation vector at the step k + 1, as well as the cross-covariance matrix $\widetilde{\boldsymbol{P}}^{\boldsymbol{\theta y}}_{1:k+1|k}$.
(7) Calculate the Kalman gain matrix $\boldsymbol{K}_{1:k+1}$ at step k + 1 from Equation (22).
(8) Update the structural parameter state vector $\widehat{\boldsymbol{\theta}}_{k+1|k+1}$ using Equation (23), and update the error covariance $\widehat{\boldsymbol{P}}^{\boldsymbol{\theta\theta}}_{k+1|k+1}$ of the state using Equation (24).
(9) Perform the next recursive calculation.

3. Numerical validation

As shown in **Figure 1**, a three-dimensional three-story frame model [11] is selected to verify the proposed method. The height of the frame is 3.66 m, and the span width is 9.14 m.

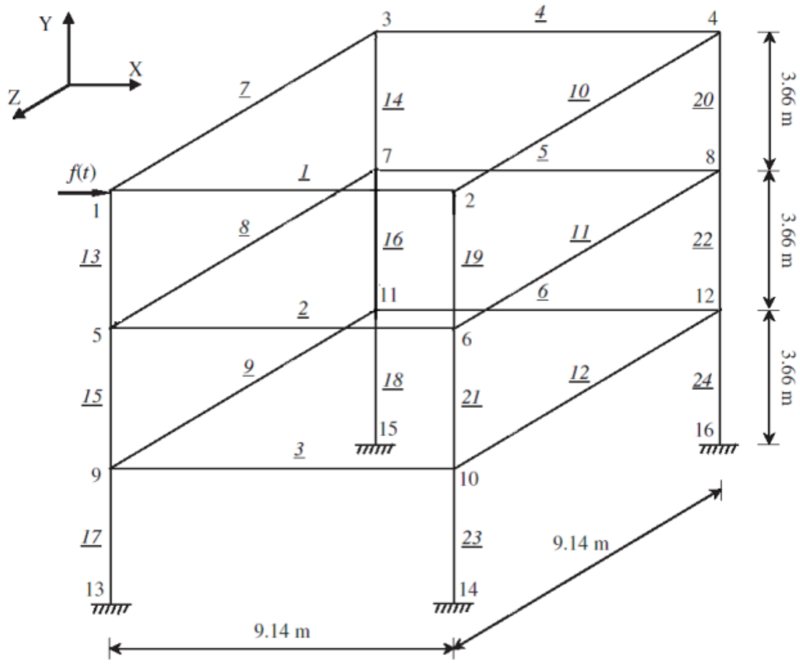

Figure 1. 3D three-tier space frame.

The frame is composed of 12 column elements and 12 beam elements. The beams and columns are made of section steel. This structure is modeled using 24 elements and 16 nodes. Among them, nodes 13, 14, 15, and 16 are fixed constraints. For three-dimensional structures, a single frame node has six degrees of freedom. Each of the remaining 12 nodes has 6 degrees of freedom, namely 3 translational degrees of freedom along the X, Y, and Z axes and 3 rotational degrees of freedom around the X, Y, and Z axes. Therefore, the entire frame has 72 degrees of freedom.

Rayleigh damping is adopted, and the Rayleigh damping coefficients are $\alpha = 0.0620$ and $\beta = 0.0145$ respectively.

The element mass matrix and element stiffness matrix of the three-dimensional frame structure are obtained by the following formula:

$$\overline{\boldsymbol{M}}_q = \frac{\bar{m}_q L_q}{420}\begin{bmatrix} 140 & 0 & 0 & 0 & 0 & 0 & 70 & 0 & 0 & 0 & 0 & 0 \\ 0 & 156 & 0 & 0 & 0 & 22L_q & 0 & 54 & 0 & 0 & 0 & -13L_q \\ 0 & 0 & 156 & 0 & -22L_q & 0 & 0 & 0 & 54 & 0 & 13L_q & 0 \\ 0 & 0 & 0 & 140a_q & 0 & 0 & 0 & 0 & 0 & 70a_q & 0 & 0 \\ 0 & 0 & -22L_q & 0 & 4L_q^2 & 0 & 0 & 0 & -13L_q & 0 & -3L_q^2 & 0 \\ 0 & 22L_q & 0 & 0 & 0 & 4L_q^2 & 0 & 13L_q & 0 & 0 & 0 & -3L_q^2 \\ 70 & 0 & 0 & 0 & 0 & 0 & 140 & 0 & 0 & 0 & 0 & 0 \\ 0 & 54 & 0 & 0 & 0 & 13L_q & 0 & 156 & 0 & 0 & 0 & -22L_q \\ 0 & 0 & 54 & 0 & -13L_q & 0 & 0 & 0 & 156 & 0 & 22L_q & 0 \\ 0 & 0 & 0 & 70a_q & 0 & 0 & 0 & 0 & 0 & 140a_q & 0 & 0 \\ 0 & 0 & 13L_q & 0 & -3L_q^2 & 0 & 0 & 0 & 22L_q & 0 & 4L_q^2 & 0 \\ 0 & -13L_q & 0 & 0 & 0 & -3L_q^2 & 0 & -22L_q & 0 & 0 & 0 & 4L_q^2 \end{bmatrix} \tag{25}$$

$$\overline{\boldsymbol{K}}_q = \bar{k}_q\begin{bmatrix} A_q/I_{zq} & 0 & 0 & 0 & 0 & 0 & -A_q/I_{zq} & 0 & 0 & 0 & 0 & 0 \\ 0 & 12/L_q^2 & 0 & 0 & 0 & 6/L_q & 0 & -12/L_q^2 & 0 & 0 & 0 & 6/L_q \\ 0 & 0 & 12b_q/L_q^2 & 0 & -6b_q/L_q & 0 & 0 & 0 & -12b_q/L_q^2 & 0 & -6b_q/L_q & 0 \\ 0 & 0 & 0 & c_q & 0 & 0 & 0 & 0 & 0 & -c_q & 0 & 0 \\ 0 & 0 & -6b_q/L_q & 0 & 4b_q & 0 & 0 & 0 & 6b_q/L_q & 0 & 2b_q & 0 \\ 0 & 6/L_q & 0 & 0 & 0 & 4 & 0 & -6/L_q & 0 & 0 & 0 & 2 \\ -A_q/I_{zq} & 0 & 0 & 0 & 0 & 0 & A_q/I_{zq} & 0 & 0 & 0 & 0 & 0 \\ 0 & -12/L_q^2 & 0 & 0 & 0 & -6/L_q & 0 & 12/L_q^2 & 0 & 0 & 0 & -6/L_q \\ 0 & 0 & -12b_q/L_q^2 & 0 & 6b_q/L_q & 0 & 0 & 0 & 12b_q/L_q^2 & 0 & 6b_q/L_q & 0 \\ 0 & 0 & 0 & -c_q & 0 & 0 & 0 & 0 & 0 & c_q & 0 & 0 \\ 0 & 0 & -6b_q/L_q & 0 & 2b_q & 0 & 0 & 0 & 6b_q/L_q & 0 & 4b_q & 0 \\ 0 & 6/L_q & 0 & 0 & 0 & 2 & 0 & -6/L_q & 0 & 0 & 0 & 4 \end{bmatrix}, \tag{26}$$

where the subscript *q* represents the *q*-th element. $\bar{m}_q$ is the mass per unit length of the *q*-th element. $\bar{k}_q = E_q I_{zq}/L_q$ is the element line stiffness, where E_q, I_{zq} and L_q are the elastic modulus, moment of inertia, and element length of the q th element, respectively, and A_q is the cross-sectional area of the *q*-th element. $a_q = I_{\bar{m}q}/\bar{m}_q$, $b_q = I_{yq}/I_{zq}$, $c_q = J_q\left[2(1+\upsilon)I_{zq}\right]$, where $I_{\bar{m}q}$, I_{yq} and J_q are the polar moment of inertia, sectional moment of inertia, and moment of inertia about mass respectively, and υ is the Poisson's ratio of the material.

The structural parameter vector to be identified is $\boldsymbol{\theta} = [k_1, \ldots\ldots, k_{24}, \alpha, \beta]^T$, so the dimension of the state vector is 26, and the initial value is selected as 0.8 times the true value. Wideband white noise excitation is applied in the direction of the X axis of node 1, as shown in **Figure 1**. The displacement response in the X direction is measured at node 1; the acceleration responses in the X direction are measured at nodes 1, 2, 4, 5, 6, 7, 8, 9, 10, 11, and 12; and the rotational acceleration responses about the X axis are measured at nodes 3, 7, 8, 10, 11, and 12. All the measured responses are contaminated by Gaussian white noise with a mean of 0, and the root mean square noise signal ratio is 2%.

The traditional UKF-UI requires the construction of an augmented state vector by incorporating structural displacements, velocities, and the structural parameters to be identified. For this three-dimensional framework structure, the dimension of the state vector is 170, including 72 displacements, 72 velocities, 24 stiffness parameters, and two damping parameters. However, the number of observed responses is only 17. This would encounter ill-conditioned problems when solving the inverse problem. The proposed algorithm of hidden state can effectively avoid the problem.

Figure 2 shows the convergence curves of the identified stiffness parameters. Due to the limited space of the paper, only the convergence curves of the stiffness parameters of the 1st, 7th, 15th, and 22nd elements are presented. It can be seen from the figure that the identified values of the stiffness of each element all show a dynamic process of gradually approaching the true stiffness parameter values.

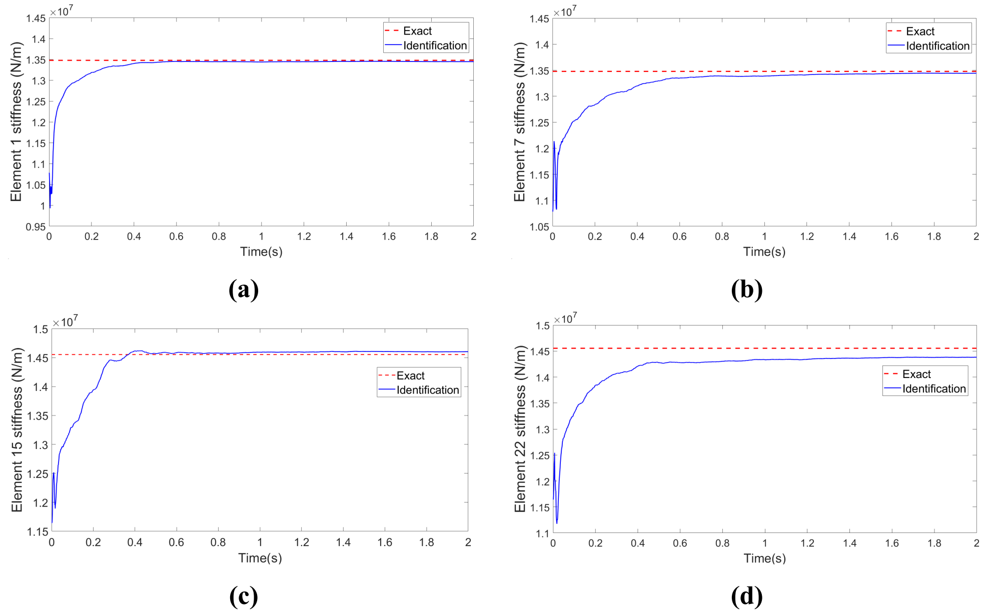

Figure 2. Convergence of element stiffness: **(a)** Element 1; **(b)** Element 7; **(c)** Element 15; **(d)** Element 22.

The convergence of the stiffness parameters is highly consistent across different elements. The identified stiffness values show obvious short-term fluctuations at the initial stage of the identification. This phenomenon is caused by the initial deviation of structural parameters (0.8 times the true value) and the accumulation of initial measurement noise errors. The algorithm needs to continuously update the parameter state vector through the unscented transform and Kalman gain correction to reduce the deviation from the true value, resulting in temporary large fluctuations of the identified values. In the steady approaching stage, the identified stiffness values gradually reduce fluctuations and show a monotonic steady trend toward the true value. At this stage, the Kalman filter recursion continuously optimizes the structural parameter state vector based on the newly obtained observation data, and the error covariance matrix of the state vector is continuously reduced, making the parameter update more stable and the identified values rapidly approaching the true value. In the stable convergence stage, the identified stiffness values converge to the vicinity of the true value, indicating that the algorithm has good stable convergence characteristics. The two damping coefficients show convergence characteristics with stiffness parameters, but have obvious differences in fluctuation range and convergence speed. The fluctuation range of α is significantly larger than that of β. This is due to the different physical sensitivities of the two damping coefficients to structural dynamic responses.

Table 1 shows the identification results and identification errors of the stiffness parameters of the three-dimensional frame structure. The overall identification effect is good, and the maximum identification error does not exceed 3.99%.

Table 1. Identification results of 3D frame stiffness parameters.

Unit number	True value (10^7 N/m)	Identified value (10^7 N/m)	Relative error (%)	Unit number	True value (10^7 N/m)	Identified value (10^7 N/m)	Relative error (%)
1	1.3476	1.3446	−0.23	13	1.4553	1.4627	0.51
2	1.3476	1.3335	−1.04	14	1.4553	1.4535	−0.13
3	1.3476	1.3179	−2.20	15	1.4553	1.4602	0.34
4	1.3476	1.3391	−0.63	16	1.4553	1.4316	−1.63
5	1.3476	1.3144	−2.46	17	1.4553	1.4507	−0.32
6	1.3476	1.4014	3.99	18	1.4553	1.4677	0.85
7	1.3476	1.3441	−0.26	19	1.4553	1.4554	0.00
8	1.3476	1.3616	−1.04	20	1.4553	1.4654	0.69
9	1.3476	1.3438	−0.28	21	1.4553	1.4456	−0.66
10	1.3476	1.3327	−1.10	22	1.4553	1.4380	−1.19
11	1.3476	1.3275	−1.49	23	1.4553	1.4449	−0.71
12	1.3476	1.3487	0.08	24	1.4553	1.4162	−2.69

To investigate the sensitivity of the hidden-state UKF-UI method to the initial values of structural parameters and verify its robustness, additional numerical experiments are designed. **Figure 3** shows identification results of different elements' stiffness parameters under the initial deviation of 0.7 times the true value. The identification accuracy is not much affected. However, if the initial deviation is large, e.g., 0.4 times the true value, the identification would not converge to the true values.

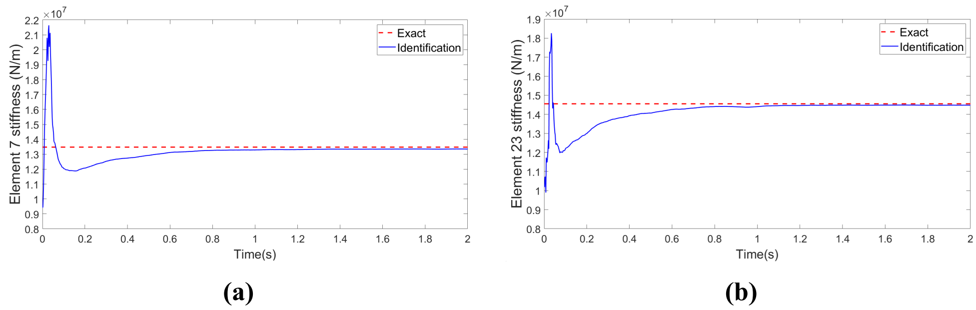

Figure 3. Identification of element stiffness under the initial deviation of 0.7 true value: **(a)** Element 7; **(b)** Element 23.

Figure 4 shows identification results of different elements' stiffness parameters under the noise level of 5% RMS. The identified structural parameters can still stably converge to the vicinity of the true values, with no obvious divergence or large deviation. The maximum relative error of stiffness parameters is less than 5%. Although the relative error has slightly increased and the convergence speed has slowed down, it is still within the allowable range for the engineering application. But for a 10% large noise level, the identification errors also increase.

Figure 5 shows the time history of the identified damping coefficients. It can be seen that β experiences a large fluctuation at the beginning of the identification, gradually approaches the true value after 0.1 s, and converges above the true value after 0.5 s; α has large fluctuations during the time from the start of the identification to 1.2 s, but gradually approaches the true value after 1.2 s and finally converges above the true value.

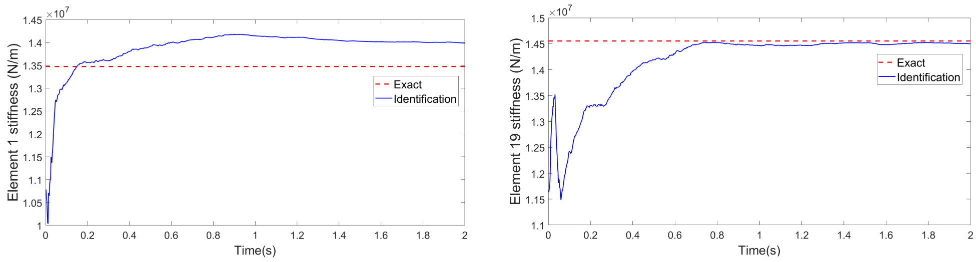

(a) **(b)**

Figure 4. Identification of element stiffness under 5% noise: **(a)** Element 1; **(b)** Element 19.

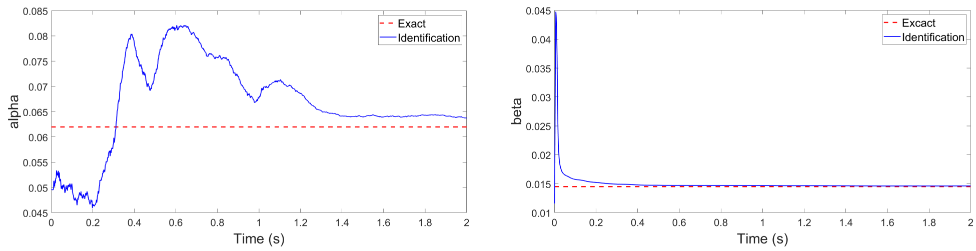

(a) **(b)**

Figure 5. Convergence curves of damping coefficients: **(a)** Damping coefficient α; **(b)** Damping coefficient β.

The two damping coefficients show consistent convergence characteristics with stiffness parameters but have obvious differences in fluctuation range and convergence speed. The fluctuation range of α is significantly larger than that of β. This is due to the different physical sensitivities of the two damping coefficients to structural dynamic responses. β is stiffness-proportional and has a strong correlation with the stiffness parameter identification results. Its convergence is driven by the accurate identification of stiffness parameters and has a smaller initial fluctuation. α is mass-proportional and is mainly sensitive to the acceleration response, which is more affected by measurement noise. It needs a longer time to eliminate noise interference and achieve stable convergence.

Table 2 shows the identification results and identification errors of the damping coefficient. The identification error of α is 2.74%, and the identification error of β is only 0.69%.

Table 2. Identification results of damping coefficient of 3D frame.

Name	True value	Identified value	Relative error (%)
α	0.0620	0.0637	2.74
β	0.0145	0.0146	0.69

Figure 6 shows the comparison between the entire true external excitation and the identified unknown excitation time history. It can be seen that the true external excitation and the identified unknown excitation are in good agreement.

Figure 7 shows the comparison between the true external excitation and the identified unknown excitation time history from 0.3 s to 0.5 s. It can be seen that there is only a very small identification deviation in the peak part. Overall, the identified unknown input time history agrees well with the true external excitation time history.

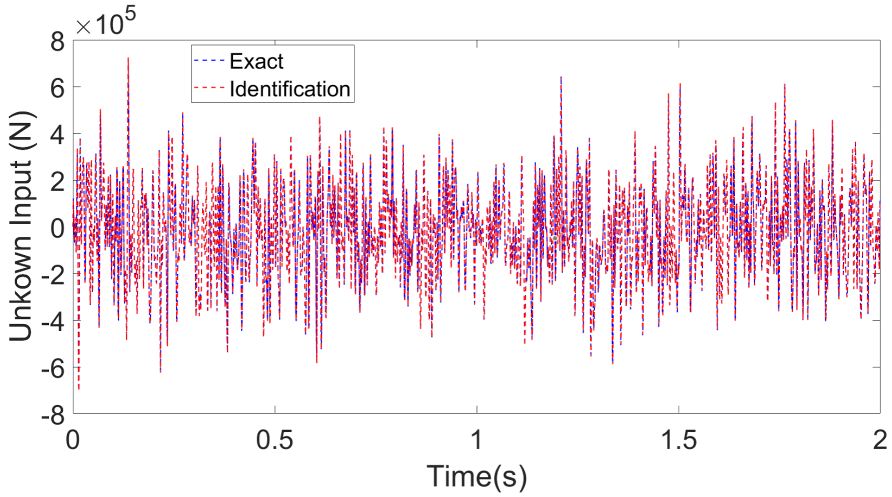

Figure 6. Comparison of time history between real external excitation and unknown excitation (0 s–2 s).

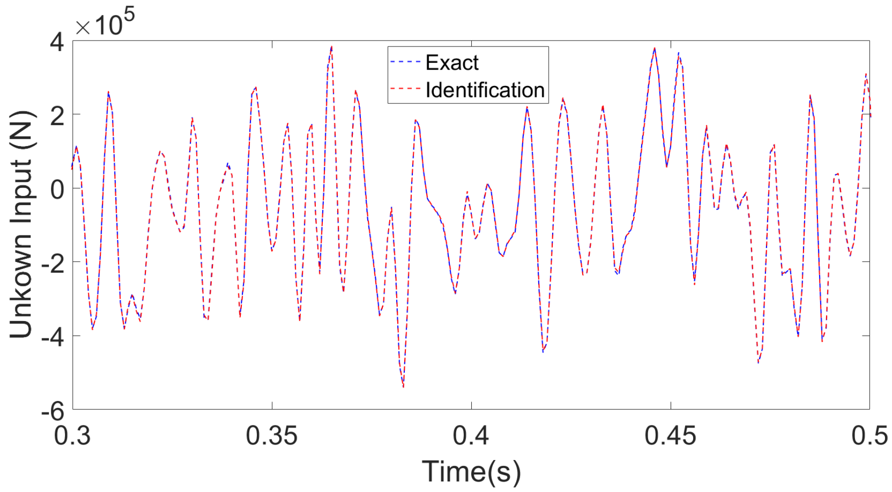

Figure 7. Comparison of time history between real external excitation and unknown excitation (0.3 s–0.5 s).

From the numerical verification results of this section, it can be seen that the hidden-state UKF-UI algorithm has high practical implication value in engineering applications. The algorithm only takes time-invariant structural parameters as the state vector, which fundamentally reduces the dimensionality of the extended state vector. This characteristic makes the algorithm suitable for real-time online identification of large-scale 3D structures, such as high-rise frame structures, spatial grid structures, and long-span bridge deck systems. In engineering practice, the algorithm can be embedded into the SHM system of such structures, and realize the real-time joint identification of structural physical parameters and unknown dynamic excitation, such as wind load, traffic load, and random seismic excitation. The identification results can directly reflect the structural damage state and the external load action characteristics, providing real-time data support for the safety early warning of the structure. In addition, the method only requires partial response measurement data for identification. This characteristic further improves the engineering practicability of the algorithm and reduces the cost of sensor layout and data collection in actual applications.

4. Conclusion

For three-dimensional multi-degree-of-freedom structural systems, a hidden-state unknown-input unscented Kalman filter is proposed for the joint identification of structural parameters and unknown excitations. By treating the displacement and velocity responses at all degrees of freedom of the three-dimensional structure as hidden states, the proposed method reduces the dimension of the state vector and becomes applicable to parameter identification of three-dimensional multi-degree-of-freedom structures. Moreover, the unbiased minimum variance estimation is used to identify unknown excitations without making any assumptions about the unknown excitation.

The effectiveness of the proposed method is verified by the identification of a three-dimensional three-story frame with 72 degrees of freedom and an unknown excitation:

(1) The identified values of the 24 stiffness parameters converge to their true values, and the maximum identification error is less than 4.0%. The identification results of the two damping parameters are also good. The identification error of damping parameter α is 2.74%, and the identification error of damping parameter β is 0.69%.
(2) Except for a very small error in the peak part, the identified unknown input matches well with the true external excitation as a whole.

The numerical identification results demonstrated that the proposed hidden-state UKF-UI identification method can effectively identify structural parameters and unknown excitation of three-dimensional structures.

This paper still requires further improvement in the following aspects:

(1) Due to the limited research time and experimental conditions, the method proposed in the paper has only been verified numerically, and no certain experiments have been conducted to verify the proposed method.
(2) The noise level studied in this study is relatively low. For joint identification under high noise conditions, further discussion and research are needed.

Author contributions: Conceptualization, LL, YL and NG; methodology, YL and YZ; software, SC and SW; validation, LL and YL; formal analysis, SC and SW; investigation, YY; resources, YL and YZ; data curation, LL; writing—original draft preparation, YY and SC; writing—review and editing, YY; visualization, YY; supervision, YL; project administration, YL and NG; funding acquisition, LL. All authors have read and agreed to the published version of the manuscript.

Funding: This work was supported by the National Natural Science Foundation of China via Grant No. 52578380.

Institutional review board statement: Not applicable.

Informed consent statement: Not applicable.

Data availability statement: The data are available from the authors upon reasonable request.

Conflict of interest: The authors declare that they have no known competing financial interests or personal relationships that could have appeared to influence the work reported in this paper.

AI use statement: The authors declare that no artificial intelligence (AI) tools were used in the preparation of this manuscript.

References

1. Sohn H, Farrar CR, Hemez FM, et al. A review of structural health monitoring literature: 1996–2001. Los Alamos National Laboratory. 2003; 1(16). Available online: https://scispace.com/pdf/a-review-of-structural-health-review-of-structural-health-285o72kjj9.pdf
2. Zar A, Hussain Z, Akbar M, et al. Towards vibration-based damage detection of civil engineering structures: Overview, challenges, and future prospects. International Journal of Mechanics and Materials in Design. 2024; 20(3): 591–662. doi: 10.1007/s10999-023-09692-3
3. Hoshiya M, Saito E. Structural Identification by Extended Kalman Filter. Journal of Engineering Mechanics. 1984; 110(12): 1757–1770. doi: 10.1061/(ASCE)0733-9399(1984)110:12(1757)
4. Liu M, Peng Z, Dong Q. Structural Damage Identification Based on Extended Kalman Filter and Response Reconstruction. Iranian Journal of Science and Technology, Transactions of Civil Engineering. 2023; 47(5): 2673–2687. doi: 10.1007/s40996-023-01101-1
5. Zhang M, Chen H, Yan T, et al. Research on improved modal parameter identification method using Hilbert-Huang transform. Measurement and Control. 2023; 56(9–10): 1637–1648. doi: 10.1177/00202940231173752
6. Zhao J, Zhou Z, Guan D, et al. Structural edge damage detection based on wavelet transform and immune genetic algorithm. Scientific Reports. 2025; 15(1): 4376. doi: 10.1038/s41598-025-87712-2
7. Chen J, Loh C. Two-stage damage detection algorithms of structure using modal parameters identified from recursive subspace identification. Earthquake Engineering & Structural Dynamics. 2018; 47(3): 573–593. doi: 10.1002/eqe.2980
8. Yu X, Li X, Bai Y. Evaluating maximum inter-story drift ratios of building structures using time-varying models and Bayesian filters. Soil Dynamics and Earthquake Engineering. 2022; 162: 107496. doi: 10.1016/j.soildyn.2022.107496
9. Kalman RE. A new approach to linear filtering and prediction problems. Journal of Basic Engineering. 1960; 82(1): 35–45. Available online: https://www.unitedthc.com/DSP/Kalman1960.pdf
10. Wei D, Li D, Huang J. Improved force identification with augmented Kalman filter based on the sparse constraint. Mechanical Systems and Signal Processing. 2022; 167: 108561. doi: 10.1016/j.ymssp.2021.108561
11. Zhang X, Luo R, He J, et al. Identification of Damping Ratios of Long-Span Bridges Using Adaptive Modal Extended Kalman Filter. Structural Control and Health Monitoring. 2025; 2025(1): 1493319. doi: 10.1155/stc/1493319
12. Yang JN, Pan S, Huang H. An adaptive extended Kalman filter for structural damage identifications II: Unknown inputs. Structural Control and Health Monitoring. 2007; 14(3): 497–521. doi: 10.1002/stc.171
13. He J, Huang Q, Xu YL. Synthesis of vibration control and health monitoring of building structures under unknown excitation. Smart Materials and Structures. 2014; 23(10): 105025. doi: 10.1088/0964-1726/23/10/105025
14. He J, Xu YL, Zhan S, et al. Structural control and health monitoring of building structures with unknown ground excitations: Experimental investigation. Journal of Sound and Vibration. 2017; 390: 23–38. doi: 10.1016/j.jsv.2016.11.035
15. Huang J, Lei Y, Li X. An adaptive generalized extended Kalman filter for real-time identification of structural systems, state and input based on sparse measurement. Nonlinear Dynamics. 2024; 112(7): 5453–5476. doi: 10.1007/s11071-023-09251-7
16. Lei Y, Qi C, Wang S. A Smoothing EKF-UI-WDF Method for Simultaneous Identification of Structural Systems and Unknown Seismic Inputs without Direct Feedthrough. Structural Control and Health Monitoring. 2023; 2023: 1–16. doi: 10.1155/2023/6968598
17. Zhang X, He J, Hua X, et al. Simultaneous Identification of Time-Varying Parameters and External Loads Based on Extended Kalman Filter: Approach and Validation. Structural Control and Health Monitoring. 2023; 2023: 1–18.

doi: 10.1155/2023/8379183

18. Julier SJ, Uhlmann JK, Durrant-Whyte HF. A new approach for filtering nonlinear systems. In: Proceedings of the 1995 American Control Conference; 21–23 June; Seattle, WA, USA. pp. 1628–1632. doi: 10.1109/ACC.1995.529783
19. Julier SJ, Uhlmann JK. New extension of the Kalman filter to nonlinear systems. In: Proceedings of the AeroSense ’97; 28 July 1997; Orlando, FL, USA. p. 182. doi: 10.1117/12.280797
20. Ding Y, Zhao BY, Wu B, et al. Simultaneous Identification of Structural Parameter and External Excitation with an Improved Unscented Kalman Filter. Advances in Structural Engineering. 2015; 18(11): 1981–1998. doi: 10.1260/1369-4332.18.11.1981
21. Al-Hussein A, Haldar A. Structural damage prognosis of three-dimensional large structural systems. Structure and Infrastructure Engineering. 2017; 13(12): 1596–1608. doi: 10.1080/15732479.2017.1304430
22. Guo LN, Ding Y, Wang Z, et al. A dynamic load estimation method for nonlinear structures with unscented Kalman filter. Mechanical Systems and Signal Processing. 2018; 101: 254–273. doi: 10.1016/j.ymssp.2017.07.047
23. Zheng ZP, Qiu H, Xia DD, et al. A Novel Unscented Kalman Filter With Unknown Input. Engineering Mechanics. 2019; 36(6): 29–35, 48. (in Chinese)
24. Lei Y, Li X, Huang J, et al. Simultaneous Assessment of Damage and Unknown Input for Large Structural Systems by UKF-UI. Journal of Engineering Mechanics. 2021; 147(10): 04021080. doi: 10.1061/(ASCE)EM.1943-7889.0001981
25. Astroza R, Ebrahimian H, Li Y, et al. Bayesian nonlinear structural FE model and seismic input identification for damage assessment of civil structures. Mechanical Systems and Signal Processing. 2017; 93: 661–687. doi: 10.1016/j.ymssp.2017.01.040
26. Castiglione J, Astroza R, Eftekhar Azam S, et al. Auto-regressive model based input and parameter estimation for nonlinear finite element models. Mechanical Systems and Signal Processing. 2020; 143: 106779. doi: 10.1016/j.ymssp.2020.106779
27. Song W. Generalized minimum variance unbiased joint input-state estimation and its unscented scheme for dynamic systems with direct feedthrough. Mechanical Systems and Signal Processing. 2018; 99: 886–920. doi: 10.1016/j.ymssp.2017.06.032